Published in final edited form as:

J Immunol. 2010 June 1; 184(11): 6242–6248. doi:10.4049/jimmunol.1000507.

Switch Region Identity Plays an Important Role in Ig Class Switch Recombination

Palash Bhattacharya[1], **Robert Wuerffel**[1], and **Amy L. Kenter**

Department of Microbiology and Immunology, University of Illinois College of Medicine, Chicago, IL 60612

Abstract

Ig class switch recombination (CSR) is regulated through long-range intrachromosomal interactions between germline transcript promoters and enhancers to initiate transcription and create chromatin accessible to activation-induced deaminase attack. CSR occurs between switch (S) regions that flank Cμ and downstream C_H regions and functions via an intrachromosomal deletional event between the donor Sμ region and a downstream S region. It is unclear to what extent S region primary sequence influences differential targeting of CSR to specific isotypes. We address this issue in this study by generating mutant mice in which the endogenous Sγ3 region was replaced with size-matched Sγ1 sequence. B cell activation conditions are established that support robust γ3 and γ1 germline transcript expression and stimulate IgG1 switching but suppress IgG3 CSR. We found that the Sγ1 replacement allele engages in μ→γ3 CSR, whereas the intact allele is repressed. We conclude that S region identity makes a significant contribution to CSR. We propose that the Sγ1 region is selectively targeted for CSR following the induction of an isotype-specific factor that targets the S region and recruits CSR machinery.

Class switch recombination (CSR) promotes diversification of IgH effector functions encoded in constant (C_H) regions while maintaining the original Ag-binding specificity arising from V(D)J recombination. The mouse IgH (*Igh*) locus contains eight C_H genes (μ, δ, γ3, γ1, γ2a, γ2b, ε, and α) that are located downstream of the V, D, and J_H segments and each C_H region is paired with a complementary switch (S) region (with the exception of Cδ). CSR occurs between S region sequences leading to an intrachromosomal deletional rearrangement that results in the formation of composite Sμ-Sx junctions on the chromosome while the intervening genomic material is looped out and excised. Activation-induced cytidine deaminase (AID) is required for CSR (1) and initiates formation of S region-specific double-strand breaks (DSBs) that are processed through a cascade of events mediated by nonhomologous end joining (2, 3).

Address correspondence and reprint requests to Dr. Amy L. Kenter, University of Illinois College of Medicine, M/C 790, 835 South Wolcott Avenue, Chicago, IL 60612-7344. star1@uic.edu.

[1]P.B. and R.W. contributed equally to this work.

Disclosures

The authors have no financial conflicts of interest.

The online version of this article contains supplemental material.

S region transcription is a defining feature of CSR. C_H genes are organized in transcription units consisting of a noncoding intronic (I) exon, the S region, and the C_H coding regions, and germline transcripts (GLTs) initiate from an intronic promoter located upstream of each I exon and terminate 3′ of the C_H coding region (4). Downstream S regions are selectively targeted for recombination with Sμ by directed activation of I exon promoters in response to combinations of Ag or mitogen, cytokines, and costimulatory signals (4). CSR occurs between highly repetitive S regions with overall length varying from 1–12 kb (5), and length influences CSR frequency both in vivo and in vitro (6, 7). Deletion of S regions or their replacement with non-S region sequences by gene-targeting methods reduces CSR, indicating that S regions are the specialized targets in this recombination event (6, 8–10). An unresolved issue is how S regions are recognized by AID and the CSR machinery.

The question of whether S region primary sequence contributes to CSR specificity has been highly controversial. The degeneracy of the S region repeats and the absence of an identifiable recombination motif (11) have led to models in which higher order structures originating from palindromic S sequences provide the recognition code for recruitment of CSR machinery (12, 13). Indeed, murine and human S regions are G-rich on the nontemplate strand, which contributes to G4 tetraplexes (14) and R-loop formation that contain ssDNA stretches as substrate for AID deamination (15). Targeted inversion of the Sγ1 region led to R-loop loss and a significant reduction of CSR activity, indicating a physiological role for R-loops in CSR (16). Studies of stably integrated transcribed switch substrates analyzed in a single B cell line have been interpreted to suggest that primary S sequence does not play a role in targeting CSR (17). An alternative model is based on transient switch plasmid studies that indicate that S region isotypes are differentially targeted for participation in CSR (reviewed in Ref. 18). CSR on transient switch substrates is AID dependent and strictly correlated with the pattern of switching at endogenous loci (2, 19, 20). In switch substrates, a single consensus Sγ3 or Sγ1 repeat is sufficient for μ→γ3 or μ→γ1 CSR, respectively, and limited mutation of the Sγ1 consensus repeat flipped its specificity to Sγ3 (7, 19). These studies raise the intriguing possibility of a central role for S region primary sequence that may function to target AID to specific S substrates.

In the wild-type (WT) control context, IL-4 reciprocally stimulates μ→γ1 and represses μ→γ3 CSR. To examine the role of S region sequence identity in CSR, we replaced the endogenous Sγ3 region with a segment of Sγ1 and compared μ→γ3 switching efficacy on the intact and targeted γ3 locus alleles upon activation with LPS in the presence or absence of IL-4. By using three independent measurements for CSR, including a newly devised method based on digestion-circularization (DC)-PCR to measure allele-specific CSR, we directly show that the γ3 allele containing the Sγ1 replacement sequence is stimulated to switch μ→γ3 by the addition of IL-4, whereas the intact allele is repressed. Our findings demonstrate that in a physiological setting, S region sequence identity contributes to isotype selection and implies that μ→γ1 CSR is normally facilitated by an IL-4–induced factor specific for Sγ1 DNA sequence.

Materials and Methods

Construction of targeting vectors and gene targeting

To create the 5′ homology arm, a 5-kb region containing Iγ3 was PCR amplified from an *Igh* containing bacterial artificial chromosome genomic clone using Expand Long Template polymerase (Roche, Basel, Switzerland) and primers 5′-TGCTCTAGAGACTTTGTTCTTGTTAATCTGCTACCTGG-3′ and 5′-CGCGCTCGAGGAGTTTCCTATACTTCTTCCTGC-3′ (nucleotide positions 1,475,648–1,480,625, accession number AJ851868; www.ncbi.nlm.nih.gov/nuccore/126349412). The amplified fragment was digested with XhoI to generate a 3.5-kb fragment that was cloned into the XhoI site of the pLNtk targeting vector. To generate the 3′ homology arm, sequences downstream of Sγ3, including the Cγ3 exons, were PCR amplified using primers 5′-CGCGGTCGACGCGGCCGCAAGATTCAAGGAGGGCTGAGGTC-3′ and 5′-CGCGGTCGACAAACACGGCAGGGCACTGGTTG-3′ (nucleotide positions 1,484,682–1,489,641, accession number AJ851868) and cloned in the SalI site of the pLNtk vector. In both cases, PCR was carried out for 30 cycles (0.5 min at 94°C, 0.5 min at 55°C, and 3 min at 68°C with 0.2 min increments at 68°C every cycle after 20 cycles). The replacement 2-kb Sγ1 region was derived from a bacterial artificial chromosome-derived BamHI fragment (nucleotide positions 1,511,993 and 1,514,053; accession number AJ851868) that was inserted between the neo cassette and the 3′ homology arm into a Not1 site that was introduced during the cloning of the 3′ homology arm. This construct was transfected into the F1 embryonic stem (ES) cell clone. Appropriately targeted clones were identified by Southern blot analysis using a probe that hybridized upstream of the 5′ homology arm. The genomic configuration of the targeted clones was confirmed by additional Southern analysis using probes that hybridized downstream of the 3′ homology arm or to the neo^r regions. The 5′ probe (995 bp) was PCR generated with primers 5′-TGAGGAGAAATGGAGATGGCT-3′ and 5′-AGATGAGTAATTCAAGTGAAC-3′ (nucleotide positions 1,476,126–1,477,120, accession number AJ851868). The 3′ probe (1026 bp) was amplified with primers 5′-CTGGGCCACT GACAGCAGAG-3′ and 5′-AAGTCTCCAACACAATCCTC-3′ (nucleotide positions 1,490,012–1,491,037, accession number AJ851868) using a 30-cycle amplification scheme (0.5 min at 94°C, 0.5 min at 53°C, and 1 min at 72°C) and Taq polymerase (Fermentas, Burlington, Ontario, Canada). Targeted ES clones were infected with recombinant adenovirus expressing the Cre recombinase to delete the neo^r and one of the two flanking *loxP* sites. These ES clones were used in the Rag2 blastocyst system to generate chimeric mice. Mouse construction and maintenance was approved by the Institutional Animal Care and Use Committees of Children's Hospital (Boston, MA) and the University of Illinois College of Medicine (Chicago, IL).

Mice, cell culture, RT-PCR, and Southern hybridization

C57BL/6, 129, and C57BL/6 × 129 mice were purchased from The Jackson Laboratory (Bar Harbor, ME). All mice were bred and housed under specific pathogen-free conditions, and animal protocols used in this study were approved by the Institutional Animal Care Committee of the University of Illinois College of Medicine. Single-cell suspensions of splenocytes from mice 6–12-wk-old were cultured as previously described (21).

Semiquantitative RT-PCR for γ3, γ1 GLT, and *Gapd* transcripts were performed as described (21, 22). For allele-specific analysis of γ3 GLT, the primers sense (5′-GTGGATCTGAACACACACAAC-3′; nt 1107–1127; D78343, Genbank, www.ncbi.nlm.nih.gov/nuccore/1799549) located in the Iγ3 exon and antisense (5′-ACAGATGAGACTGTGCGCAC-3′; nt 6400–6381) located in γ3 C_H1 were used in PCR (0.5 min at 94°C, 0.5 min at 53°C, and 1 min at 72°C) for 33 cycles and resulted in a 384-bp product. PstI digestion of the γ3 GLT PCR products generates 180- and 125-bp restriction fragments derived from the C57/B6 (b) and 129 (a) alleles, respectively. The PCR products and restriction fragments were resolved on 2% agarose gels and were analyzed by Southern hybridization with a [^{32}P]γ-ATP–labeled oligonucleotide probe (5′-CTCAGGGAAGTAGCCTTTGACA-3′; nt 6338–6317), which is complementary to both the 129-and C57/B6-specific fragments using standard techniques. For direct visualization of the allele-specific γ3 GLTs, we used the same protocol described above except the sense primer (5′-CTGGCAGGACCAAATTCGCT-3′; nt 1231–1250) located in the Iγ3 exon was used and gave a final 260-bp PCR product as shown in Fig. 2B. Primers for postswitch transcripts (PSTs) (for μ→γ3 and μ→γ1 switching) were described (19).

Allele-specific DC-PCR

The DC-PCR assay was carried out as previously described (23, 24), with modifications. Splenocytes from WT F1 (control) or chimeric mice were cultured for 5 d in the presence of LPS or LPS plus IL-4 (1 ng/ml), and genomic DNA was isolated. Nested DC-PCR primer sets were designed to analyze C57BL/6 and 129 allele-specific μ→γ3 CSR using EcoRI digestion based on genomic sequence (accession number NT_166318, www.ncbi.nlm.nih.gov/nuccore/149263585; and AJ851868, respectively). For the 129 (a) allele, the primers for round 1 are 129SuDC.a 5′-CTTAGAAGCCCTTCACGC-3′ (nucleotide positions 1,417,670–1,417,653) and 129g3DC.a 5′-CTATGTCCAATGTTCTGAGGAATCA-3′ (nucleotide positions 1,493,471– 1,493,495) for 18 cycles (94°C for 30 s; 58°C for 30 s; and 72°C for 50 s) in a 25-μl reaction and 2.5 μl used to program round 2. The primers for round 2 are 129SuDC.b 5′-CTCTCAACCACCAACCAGCATGTTCAACC-3′ (nucleotide positions 1,417,633–1,417,605) and 129g3DC.b 5′-ACCATTCTGACTGGTGTGAGTAGA-3′ (nucleotide positions 1,493,611–1,493,634). PCR is carried out (94°C for 30 s; 65°C for 30 s; 72°C for 30 s) and 5 μl product is harvested at 26, 29, and 32 cycles. For the C57BL/6 (b) allele, the DC-PCR primers are C57Su.a 5′-GAAGCCCTTCACGTCACTGACTGACTG-3′ (nucleotide positions 25,618,223–25,618,249) and C57g3.a 5′-GCATCTGTCCTTATTACATGTTAGAG-3′ (nucleotide positions 25,544,488–25,544,463), and PCR was carried out for 15 cycles (94°C for 30 s; 58°C for 30 s; 72°C for 50 s) in a 25-μl reaction and 2.5 μl used to program round 2. The primers for round 2 are Su.b 5′-GAATGGAGACCAATAATCAGAGGGAAG-3′ (nucleotide positions 25,618,482–25,618,508) and C57g3.b 5′-GTACCAGCTTGCAATCCCACCATC-3′ (nucleotide positions 25,544,363–25,544,340). PCR is carried out (94°C for 30 s; 60°C for 30 s; 72°C for 30 s), and 5 μl product is harvested at 26, 29, and 32 cycles. Nested μ→γ1 DC-PCR primer sets were designed to specifically analyze CSR on both the C57BL/6 and 129 alleles and are based on genomic sequence for C57BL/6 (accession number NT_166318) and 129 (accession number AJ851868) and using EcoRI digestion. PCR was carried out in a 25-μl

reaction using 1.25 U hot start Platinum Taq with 2.5 mM $MgCl_2$ for both rounds 1 and 2. The primers for round 1 are Su.b 5′-GAATGGAGACCAATAATCAGAGGGAAG-3′ (AJ851868, nucleotide positions 1,417,407–1,417,381; NT_166318, nucleotide positions 25,618,482–25,618,508) and RWDCg1.a 5′-GCTACCAAG-GATCAGGGATAGAC-3′ (NT_166318, nucleotide positions 25,525,296– 25,525,274; AJ851868, nucleotide positions 1,518,352–1,518,374). PCR was carried out for 15 cycles (94°C for 30 s; 62°C for 30 s; 72°C for 35 s) and 2.5 μl used to program round 2. The primers for round 2 are Su.b and RWDCg1.b 5′-TCTCCTGGGTAGGTTACAGGT-3′ (AJ851868, nucleotide positions 1,518,562–1,518,582 and NT_166318, nucleotide positions 25,525,086–25,525,066). PCR (94°C for 30 s; 60°C for 30 s; 72°C for 20 s) products (5 μl) were harvested at 26, 29, and 32 cycles.

Cloning and DNA sequence analysis of S/S junctions

Sμ-Sγ3 and Sμ- replacement Sγ1(Sγ1^{KI}) junctions were amplified by PCR with primers SμUP.A1F 5′-GAGCTGAGATGGGTGGGCTTC-3′ (C57BL/6 accession number, NT_166318, coordinates 25,617,103–25,617,083; 129 accession number, AJ851868, coordinates 1,418,786–1,418,806) and Sγ3DS. A1R 5′-GGCTAAGCCATCTGAGTTGGCTCT-3′ (in NT_166318, coordinates 25,553,107–25,553,130 [www.ncbi.nlm.nih.gov/nuccore/149263585];in AJ851868 coordinates 1,484,787–1,484,764 [www.ncbi.nlm.nih.gov/nuccore/126349412]) for 36 cycles (95°C for 40 s; 66°C for 40 s; 72°C for 4 min plus 5 s added each cycle) in 25-μl reactions containing 2.5 mM $MgCl_2$ and 2.5 U Platinum Taq (Invitrogen, Carlsbad, CA). At least three independent reactions from two control and five experimental mice were used to obtain products. PCR products ranging from 500–3000 bp were gel purified and cloned into the TOPO-TA vector (Invitrogen). Plasmid DNAs were prepared using Perfectprep Plasmid 96 Vac Kit (5 Prime, Gaithersburg, MD) and sequenced (Applied Biosystems 3730 DNA Analyzer, Applied Biosystems, Foster City, CA). S-S junctions were determined by alignment to the National Center for Biotechnology Information and Ensembl *Igh* databases (NT_166318, AJ851868). Breakpoint positions in Sμ, Sγ3, or the knockin Sγ1 alleles are expressed as the distance from the end of the SμUP.A1F or Sγ3DS.A1R primers. Multiple polymorphisms distinguish the a and b alleles and were used to identify allele usage in CSR events. Differences in Sμ between C57BL/6 (b) and 129 (a) alleles occur at positions (C57BL/6→129) 7(T→C), 283(A→C), 339(A→G), 410 (G→A), and 430(G→A). Differences in Sγ3 between C57BL/6 (b) and 129 (a) alleles occur at positions (C57BL/6→129) 1(T→A), 2(T→C), 35(G→A), 39–41(ACC→CGT), 44–46(GAC→CTG), 48(A→G), 57(A→G), 62(A→G), 125 (A→G), 135(G→A), 197–198(GT→AC), 256(A→G), 258(G→C), and 330 (C→T).

Results

Replacement of Sγ3 with size-matched Sγ1

To clarify the function of S region identity in CSR mechanisms, we sought to determine whether physiological μ→γ1 CSR is mediated by Sγ1 sequence through an IL-4–inducible activity that is independent of GLT expression and AID. We used gene-targeted mutation techniques to exchange the endogenous Sγ3^a region and downstream flanking region with a

2-kb segment of the core Sγ1[a] in the γ3[a]/γ3[b] F1 ES cell line (Fig. 1A). This Sγ1 sequence was previously demonstrated to mediate CSR in transient switch plasmid studies (7, 19), is size matched with the endogenous Sγ3, and contains a similar number of C residues. The γ3 GLT promoter, Iγ3 exon and splice donor, and acceptors are unchanged. The F1 ES cell line derives from 129Sv-C57BL/6 mice, and the two *Igh* alleles originate from the *Igh*^{a} (from 129Sv) and the *Igh*^{b} (from C57BL/6) allotypes, respectively (16, 25). Our targeting construct was built using 129Sv DNA, and all targeting mutations were introduced into the *Igh*^{a} allele while the *Igh*^{b} allele remained in the WT configuration. In the targeting vector, the inserted Sγ1[a] is oriented in the physiological direction with respect to the germline Iγ3 promoter and contained a neomycin resistance selectable marker gene, neo[r] (Fig. 1A). Neo[r] can interfere with germline transcription from I promoters (26) and was therefore flanked by 34-bp *loxP* sequences (27) and subsequently deleted by exposure to Cre recombinase. The presence of sequence polymorphisms facilitates comparison of CSR levels on the modified *Igh*^{a} allele to that found on the unmodified *Igh*^{b} allele. The size and integrity of the inserted Sγ1[a] region was confirmed by Southern blot analyses with probes immediately flanking the 5′ and 3′ homology arms (Fig. 1B). On the targeted allele, the 6.3-kb and 12-kb EcoRI fragments are found when analyzed with the 5′ and 3′ probes, respectively. On the γ3[b] allele, an 18-kb fragment is found when analyzed with either probe. Cre deletion results in the removal of the neo gene, leaving a single *loxP* at the site. Following Cre-deletion, the 6.3-kb fragment is shortened to 4.5 kb, whereas the 12-kb fragment remains unchanged. To obtain mature B cells harboring the Sγ1 knockin allele, referred to in this study as γ3[a(KI)], the successfully targeted F1 ES cells were injected into RAG2-deficient blastocysts to generate chimeric mice.

GLT γ3 is expressed upon treatment with LPS and low-dose IL-4

A requirement for analysis of CSR in the Sγ1 replacement chimeras is activation conditions that include IL-4 and are supportive of γ3 GLT expression. Severinson and coworkers (28) have shown that LPS alone and in combination with reduced-dose IL-4 (1–10 ng/ml) synergizes to stimulate large amounts of γ3 GLT, whereas LPS and very high concentration IL-4 (20 ng/ml) suppress γ3 GLTs. We confirm in this study that γ3 GLTs are highly expressed in purified CD43$^-$ splenic B cells that are unstimulated or activated with LPS alone or LPS plus IL-4[hi] (10 ng/ml), whereas the γ1 GLTs are LPS plus IL-4 dependent, and AID is induced by either LPS or LPS plus IL-4 (Fig. 2A). A similar GLT expression profile is found for splenocytes from C57BL/6 × 129 (WT F1) and a chimera (Chi 28) that are unstimulated or activated with LPS alone, LPS plus IL-4[lo] (1 ng/ml), or LPS plus IL-4[hi], in which γ3 GLT is expressed under all three conditions, whereas the γ1 GLT is dependent on the combination of LPS plus IL4 (Fig. 2B), indicating that the culture conditions chosen for this analysis are appropriate.

Chimeric B cells produce appropriate levels of γ3 GLT in all activation conditions

WT F1 or chimeric knockin (Chi) mice were next stimulated with LPS and analyzed for γ3 GLT abundance. Allele-specific γ3 GLT RT-PCR products are distinguished using a restriction site polymorphism that uniquely creates an additional PstI site on the γ3[a] allele. Intact and PstI-digested cDNA representing γ3 GLT derived from the a (129) or b (C57BL/6) or a and b (F1) alleles are clearly distinguishable (Fig. 2C, *lanes 2–5*). RT-PCR

amplification of γ3 GLTs derived from WT F1 and three independent chimeras (Chi D, E, and F) indicates that Sγ1 region replacement had no substantial deleterious effect on GLT expression from the Iγ3 promoter, although GLT abundance from the $\gamma3^{a(KI)}$ allele appears somewhat underrepresented as compared with WT (Fig. 2C). To further examine this issue, allele-specific γ3 GLT abundance from WT F1 and Chi 1 cultures activated with LPS only, LPS plus IL-4^{lo}, or LPS plus IL-4^{hi} was assessed by RT-PCR followed by Southern blot analysis. In WT F1 samples, there is parity of γ3 GLT expression from both alleles, whereas in the Chi 1 γ3 GLT, quantities from the a allele are somewhat underrepresented as compared with the b allele for all activation conditions (Fig. 2D). These results confirm that γ3 GLTs from the intact and targeted alleles are expressed in the chimera cultures and that stimulation does not lead to overexpression of the γ3 GLT from the a allele.

Chimeric B cells express γ3 PSTs upon activation with LPS and IL-4

To further assess CSR in WT and chimeric cultures, Iμ-Cγ3 and Iμ-Cγ1 PST expression patterns, indicators of successful CSR, were analyzed by RT-PCR. In WT cultures from purified B cells or total splenocytes, μ→γ3 CSR is abolished following stimulation with LPS plus IL-4, as measured by the repression of Iμ-Cγ3 PST in comparison with activation with LPS alone (Fig. 3A, 3B). Reciprocally, the Iμ-Cγ1 PST is induced by LPS plus IL-4 as expected (Fig. 3A, 3B). The RT-PCR analysis of the *Gapd* or *Hprt* loading controls indicates that all samples are equivalently represented. It is notable that despite WT γ3 GLT and AID expression (Fig. 2A, 2B), μ→γ3 CSR is repressed when cells are treated with LPS plus IL-4 (Fig. 3A, 3B), implying that additional layers of regulation determine the outcome of isotype-targeted CSR.

Strikingly, in chimera cultures (Chi D, E, and F), γ3 PSTs were detected following induction by LPS or LPS plus IL-4, indicating that μ→γ3 CSR was active in the presence of $IL4^{lo}$ or $IL4^{hi}$, whereas γ1 PSTs were induced by LPS plus IL-4 but not by LPS alone, which verifies appropriate IL-4 activity (Fig. 3B). The PST analyses indicate that μ→γ3 CSR occurs in the chimeric cultures activated with LPS plus IL-4, conditions that normally suppress switching in the WT. These studies do not distinguish whether in the chimeras one or both γ3 alleles are involved in CSR.

LPS and IL-4 induce μ→γ3 CSR on the Sγ1 replacement allele

In WT B cells, CSR tends to occur on both *Igh* alleles and to the same isotype (29–31). Newly devised allele-specific semi-quantitative DC-PCR assays were performed to determine which γ3 allele is responsible for high levels of IgG3 expression in chimeric B cells following LPS plus IL-4 treatment. The DC-PCR strategy is diagrammed, and a portion of the *Igh* locus before and after μ→γ3 recombination is shown (Fig. 4A). CSR for μ→γ3 generates a new S/S hybrid configuration, 5′-Sμ/Sγ3-3′, in which EcoRI sites that flank the 5′ and 3′ ends of the Sμ and Sγ3 regions, respectively, are preserved. Postdigestion with EcoRI, the DNA is ligated under low concentration conditions that favor intramolecular ligation. Nested primer sets specific for sites at the 5′ end of Sμ and the 3′ end of Sγ3 amplify the region spanning the circle joint and yield a specific Sμ/Sγ3 DC-PCR product. Newly designed allele-specific DC-PCR primers amplify μ→γ3 events on the $\gamma3^{a}$ or $\gamma3^{b}$ alleles as demonstrated using DNA from 129 or C57BL/6 B cells, respectively (Fig. 4B).

The *nAChR* gene DC-PCR product functions as a control for the assay (Fig. 4B). Accumulation of DC-PCR products from both the $\gamma 3^{a}$ and $\gamma 3^{b}$ alleles is dependent on increasing cycles of amplification and is in the linear range of detection (Supplemental Fig. 1). In LPS-activated control WT F1 cells, $\mu \rightarrow \gamma 3$ CSR is almost equivalently stimulated on both the $\gamma 3^{a}$ and $\gamma 3^{b}$ alleles (Fig. 4C). Stimulation with LPS in the presence of increasing concentrations of IL-4 yields diminished $\mu \rightarrow \gamma 3$ CSR on both alleles and increased $\mu \rightarrow \gamma 1$ switching as compared with LPS alone (Fig. 4C, 4D) in agreement with the pattern of $\gamma 3$ PST expression (Fig. 3). In LPS-induced chimeric splenocyte cultures, CSR on the $\gamma 3^{a(KI)}$ allele is ~3- to 4-fold higher than for the intact $\gamma 3^{b}$ allele (Fig. 4C). Upon LPS plus IL-4 activation, there is robust switching $\mu^{a} \rightarrow \gamma 3^{a(KI)}$, whereas $\mu \rightarrow \gamma 3^{b}$ is undetectable. When Chi D templates are concentrated 5-fold, then $\mu \rightarrow \gamma 3^{b}$ DC-PCR products, denoted $\mu \rightarrow \gamma 3^{b}$*, are detectable from cells induced with LPS plus IL-4^{lo} but not with LPS plus IL-4^{hi} (Fig. 4C). These findings demonstrate that switching on the intact b allele is repressed at least 10-fold by IL-4^{lo} and to an even greater extent by IL-4^{hi} treatment, whereas CSR on the S$\gamma 1$ replacement allele is active. We also find that the level of $\gamma 3$ GLT produced from the $\gamma 3^{a(KI)}$ allele is somewhat reduced as compared with the intact $\gamma 3^{b}$ allele under identical culture conditions (Fig. 2D). Hence, the enhanced $\mu^{a} \rightarrow \gamma 3^{a(KI)}$ CSR detected when chimera cultures are activated in the presence of LPS and IL-4 may be an underestimate of CSR potential for this allele.

In cultures activated with LPS alone, the incidence of switching on the $\gamma 3^{a(KI)}$ allele was unexpectedly high (Fig. 4C) if CSR is strictly dependent on IL-4. Switching $\mu \rightarrow \gamma 1$ in response to LPS alone was higher in chimera as compared with WT cultures, suggesting the presence of some endogenous IL-4 (Fig. 4C). To explore the possibility that endogenous IL-4 accounts for $\mu \rightarrow \gamma 3$ switching on the $\gamma 3^{a(KI)}$ allele in the LPS-activated cultures, we analyzed a fourth chimera, Chi 1, in which $\mu \rightarrow \gamma 1$ CSR was undetectable by DC-PCR when activated with LPS alone, demonstrating minimal levels of endogenous IL4 (Fig. 4D). In Chi 1, activation by LPS alone led to relatively more $\mu \rightarrow \gamma 3$ switching on the intact $\gamma 3^{b}$ allele than the S$\gamma 1$ replacement allele, whereas this pattern is reversed following induction with LPS plus IL-4^{lo}. Thus, CSR on the $\gamma 3^{a(KI)}$ allele is ~4- to 5-fold higher compared with the intact $\gamma 3^{b}$ allele poststimulation with LPS plus IL-4^{lo} and suggests dependency of the S$\gamma 1$ replacement allele on IL4 for $\mu \rightarrow \gamma 3$ switching. Irrespective of the level of IL-4 present, it is clear that the chimera cultures permit some endogenous $\mu \rightarrow \gamma 1$ CSR when activated with LPS alone. We favor the view that the chimera environment is permissive for the participation of S$\gamma 1^{KI}$ allele in CSR within the context of the $\gamma 3$ locus because of higher IL-4 levels. However, we cannot formally rule out the possibility that S$\gamma 1$ sequence is intrinsically a more robust substrate than S$\gamma 3$ when compared side by side for CSR within the same locus.

Preferential usage of the $\gamma 3^{a(KI)}$ allele in S-S junctions is induced by IL-4

To independently examine the influence of IL-4 on isotype usage during CSR, we analyzed allelic frequencies of S/S junctions that were directly amplified by PCR from control WT F1 and five independent chimeric splenocyte cultures. Splenocytes were stimulated with LPS or LPS plus IL-4^{lo} for 5 d, and genomic DNA was harvested. The PCR primers used to amplify these S/S junctions were identical in all cases (Fig. 5). DNA sequence polymorphisms

distinguish Sμ/Sγ3 junctions derived from the a and b allele (see *Materials and Methods*). Most normal CSR breakpoints occur within and just beyond the S tandem repeats (11). In WT F1 and chimeric DNAs, Sμ recombination breakpoints occurred at various positions and were fused to complementary sites within intact Sγ3 or $S\gamma1^{KI}$ alleles (Fig. 5A). S/S junctions from chimeric cultures were generally focused to the 5′ region of Sμ and the 3′ region of $S\gamma3^{b}$ and $S\gamma1^{KI}$, sequences similar to the pattern found for WT Sμ and Sγ3 fusion sites (Fig. 5B). Sμ/Sγ3 recombination junctions carried insertions, deletions, and mutations typical of S/S junctions, and only unique junctions were considered (Supplemental Figs. 2, 3). In WT F1 controls, similar numbers of $S\mu^{a}/S\gamma3^{a}$ and $S\mu^{b}/S\gamma3^{b}$ junctions were isolated following activation with LPS or LPS plus IL-4^{lo}, indicating the equivalent usage of the a and b alleles in CSR (Table I). Similarly, in LPS-activated splenocyte cultures from Sγ1 replacement chimeras, the distribution of S/S junctions was well balanced between the intact $S\mu^{b}/S\gamma3^{b}$ and replacement $S\mu^{a}/S\gamma1^{KI}$ alleles. Strikingly, when these cultures are stimulated with LPS plus IL-4^{lo}, the frequency of $S\mu^{a}/S\gamma1^{KI}$ junctions is significantly overrepresented ($p > 0.011$), demonstrating that upon LPS activation, IL-4 signaling facilitates CSR targeted to Sγ1 sequences even when in the context of the γ3 locus (Table I).

Discussion

We replaced the endogenous Sγ3 region with Sγ1 DNA by gene targeting to determine whether S region sequence identity plays a role in focusing CSR to specific isotypes. Because CSR is critically dependent on GLT expression, we established conditions in which γ3 GLTs from both the intact and Sγ1 replacement loci are well expressed even in the presence of IL-4, in agreement with previous studies (28). Successful expression of γ3 GLTs on both alleles allowed us to determine whether the Sγ1 replacement allele is preferentially targeted for μ→γ3 switching in the presence of IL-4. In LPS-activated WT splenocyte cultures, μ→γ3 events diminish on both alleles as a function of increasing IL-4 concentration as detected in PST assays, in allele-specific DC-PCR, and in S/S junction frequency studies, whereas, in chimeric splenocytes, IL-4 stimulation induces γ3 PST expression coupled with preferential usage of the $\gamma3^{a(KI)}$ allele in μ→γ3 events as directly visualized in DC-PCR analyses and reflected in S/S junction frequency assays. These findings suggest that $\gamma3^{a(KI)}$ effectively competes with the $\gamma1^{a}$ locus for CSR machinery as a consequence of IL-4 stimulation. In summary, when chimeric B cells are activated with LPS and IL-4, the Sγ1 replacement sequence becomes a high-efficiency substrate in μ→γ3 switching in contrast to the intact allele, which ceases to engage in CSR. This finding is even more striking given the relatively lower level of γ3 GLT from the $\gamma3^{a(KI)}$ allele as compared with the intact allele and demonstrates a role for primary S region sequence in CSR.

The Sγ1 replacement allele was capable of supporting some CSR in response to LPS alone. There are several possible explanations for this observation. Our studies show that low levels of endogenous IL-4 were present in the splenocyte cultures, which could account for participation of the $\gamma3^{a(KI)}$ allele in μ→γ3 CSR. There may be cryptic sequences within the residual Sγ3-Cγ3 intronic region that confer the ability to recombine in response to LPS alone. Transcribed S regions contain R loops that are dependent on the presence and orientation of the S region (8, 15, 32). Deletion of endogenous Sγ1 essentially abolished μ→γ1 CSR, but knockin of a random synthetic G-rich sequence that was also capable of

transcription-dependent R-loop formation provided nearly 10% of CSR as compared with WT CSR activity (8). Therefore, any transcribed DNA sequence situated in the Iγ3-Cγ3 intron that forms R-loops, such as the Sγ1 replacement sequence, may function as a low-efficiency substrate for CSR in response to LPS stimulation.

CSR is mediated by AID attack, resulting in DSB formation in Sμ and a downstream S region, long-range synapsis between targeted S regions and joining of DSBs by constituents of the nonhomologous end joining pathway (2, 3, 21). How might S region sequence identity influence CSR targeting in vivo? One potential explanation is that Sγ1 is simply a better target for CSR. If this were so when holding GLT expression constant, then the differential CSR frequency between Sγ3 and Sγ1 will remain equivalent under all activation conditions. We find the converse, that preferential usage of the Sγ1 replacement allele is IL-4 dependent, demonstrating that Sγ1 is not simply a better substrate for switching but rather differentially targeted for CSR under those conditions. Our data are not inconsistent with the notion that Sγ1 might be a better substrate for CSR than Sγ3 and also be facilitated in CSR by an IL-4–inducible process. Additional studies using a germline $S\gamma1^{KI}$ allele in mice will be required to resolve this issue. Another question posed by our studies is whether the influence of Sγ1 sequence identity on CSR can be generalized to all isotypes. It is notable that the overall mechanism of CSR is the same for Sγ1 as for other isotypes. However, in B cells harboring a deletion of hs3b,4, a critical component of 3′ Eα, some μ→γ1 switching is detected, whereas all other isotypes are inert (33). Chromatin conformation capture studies demonstrate that in the hs3b,4 deleted B cells activated with LPS plus IL-4, the γ1 locus is uniquely capable of some interaction with Eμ, thereby creating Sμ/Sγ1 proximity (21). Thus, it is possible that when triggered by IL-4, the Sγ1 replacement allele is inherently better at synapsis with Sμ, leading to enhanced CSR frequencies. S/S junctions are created by joining DSBs in Sμ with those of a distal S region by means of DSB repair proteins, including the catalytic subunit of the DNA-dependent protein kinase (DNA-PKcs). Although CSR is profoundly reduced in DNA-PKcs–deficient B cells, some μ→γ1 switching survives (34), perhaps indicating that Sγ1 is more facile than other S regions in the joining reaction. Alternatively, detection of residual μ→γ1 CSR in hs3b,4 deleted- or DNA-PKcs–deficient B cells might be a byproduct of assay sensitivity because μ→γ1 CSR normally occurs at a higher frequency relative to other isotypes. Our studies do not directly distinguish whether the Sγ1 replacement allele is preferentially targeted by AID or preferentially involved in synapsis with Sμ or is a better substrate for end joining as compared with Sγ3. Nevertheless, our findings demonstrate that S region sequence identity plays a role in CSR, and the effect is dependent on IL-4.

An intriguing explanation for our results is suggested by the findings that isotype-specific CSR occurs on switch-specific substrates in transient assays (7), and S region-specific DNA binding proteins have been detected (reviewed in Ref. 18). Together, these studies imply that recognition motifs in S regions interact with DNA binding proteins to recruit the CSR machinery. In this context, it is possible that a factor specific for the Sγ1 replacement allele is induced (or a repressor is repressed) by IL-4 in LPS-activated B cells and promotes μ→γ1 CSR. An independent gene-targeting study showed that a Sγ3 replacement allele within the endogenous γ1 locus supported CSR following B cell activation with LPS plus IL-4 (35). This observation was predicted by switch substrate studies in which μ→γ3 CSR was

stimulated by LPS but not repressed by IL-4 (7). Alternatively, the Sγ3 replacement study could mean that any S region is capable of supporting CSR with the exception of Sγ1, which is a special case. Additional work is required to investigate the step at which S region sequence identity functions in the CSR reaction, whether Sγ1 is unique among S regions, and whether isotype-specific factors are involved in this process.

Supplementary Material

Refer to Web version on PubMed Central for supplementary material.

Acknowledgments

We thank Drs. Alt and Zarrin for help generating the chimeras and Y Fujiwara, T. Borjeson, and A. Riley for performing ES cell injections.

This work was supported by the National Institutes of Health (AI052400 to A.L.K.).

Abbreviations used in this paper

AID	activation-induced deaminase
Chi	chimeric knockin
CSR	class switch recombination
DC	digestion-circularization
DNA-PKcs	catalytic subunit of the DNA-dependent protein kinase
DSB	double-strand break
ES	embryonic stem
GLT	germline transcript
I	intronic
neo	neomycine resistance gene
PST	postswitch transcript
S	switch
$S\gamma1^{KI}$	replacement Sγ1
tk	gene encoding the thymidine kinase
WT	wild-type

References

1. Muramatsu M, Kinoshita K, Fagarasan S, Yamada S, Shinkai Y, Honjo T. Class switch recombination and hypermutation require activation-induced cytidine deaminase (AID), a potential RNA editing enzyme. Cell. 2000; 102:553–563. [PubMed: 11007474]

2. Kenter AL. Class switch recombination: an emerging mechanism. Curr Top Microbiol Immunol. 2005; 290:171–199. [PubMed: 16480043]
3. Chaudhuri J, Basu U, Zarrin A, Yan C, Franco S, Perlot T, Vuong B, Wang J, Phan RT, Datta A, et al. Evolution of the immunoglobulin heavy chain class switch recombination mechanism. Adv Immunol. 2007; 94:157–214. [PubMed: 17560275]
4. Stavnezer J. Molecular processes that regulate class switching. Curr Top Microbiol Immunol. 2000; 245:127–168. [PubMed: 10533321]
5. Gritzmacher CA. Molecular aspects of heavy-chain class switching. Crit Rev Immunol. 1989; 9:173–200. [PubMed: 2505810]
6. Zarrin AA, Tian M, Wang J, Borjeson T, Alt FW. Influence of switch region length on immunoglobulin class switch recombination. Proc Natl Acad Sci USA. 2005; 102:2466–2470. [PubMed: 15684074]
7. Kenter AL, Wuerffel R, Dominguez C, Shanmugam A, Zhang H. Mapping of a functional recombination motif that defines isotype specificity for mu—>gamma3 switch recombination implicates NF-kappaB p50 as the isotype-specific switching factor. J Exp Med. 2004; 199:617–627. [PubMed: 14993249]
8. Shinkura R, Tian M, Smith M, Chua K, Fujiwara Y, Alt FW. The influence of transcriptional orientation on endogenous switch region function. Nat Immunol. 2003; 4:435–441. [PubMed: 12679811]
9. Luby TM, Schrader CE, Stavnezer J, Selsing E. The mu switch region tandem repeats are important, but not required, for antibody class switch recombination. J Exp Med. 2001; 193:159–168. [PubMed: 11148220]
10. Khamlichi AA, Glaudet F, Oruc Z, Denis V, Le Bert M, Cogné M. Immunoglobulin class-switch recombination in mice devoid of any S mu tandem repeat. Blood. 2004; 103:3828–3836. [PubMed: 14962903]
11. Dunnick W, Hertz GZ, Scappino L, Gritzmacher C. DNA sequences at immunoglobulin switch region recombination sites. Nucleic Acids Res. 1993; 21:365–372. [PubMed: 8441648]
12. Manis JP, Tian M, Alt FW. Mechanism and control of class-switch recombination. Trends Immunol. 2002; 23:31–39. [PubMed: 11801452]
13. Honjo T, Kinoshita K, Muramatsu M. Molecular mechanism of class switch recombination: linkage with somatic hypermutation. Annu Rev Immunol. 2002; 20:165–196. [PubMed: 11861601]
14. Duquette ML, Handa P, Vincent JA, Taylor AF, Maizels N. Intracellular transcription of G-rich DNAs induces formation of G-loops, novel structures containing G4 DNA. Genes Dev. 2004; 18:1618–1629. [PubMed: 15231739]
15. Huang FT, Yu K, Balter BB, Selsing E, Oruc Z, Khamlichi AA, Hsieh CL, Lieber MR. Sequence dependence of chromosomal R-loops at the immunoglobulin heavy-chain Smu class switch region. Mol Cell Biol. 2007; 27:5921–5932. [PubMed: 17562862]
16. Zarrin AA, Alt FW, Chaudhuri J, Stokes N, Kaushal D, Du Pasquier L, Tian M. An evolutionarily conserved target motif for immunoglobulin class-switch recombination. Nat Immunol. 2004; 5:1275–1281. [PubMed: 15531884]
17. Kinoshita K, Harigai M, Fagarasan S, Muramatsu M, Honjo T. A hallmark of active class switch recombination: transcripts directed by I promoters on looped-out circular DNAs. Proc Natl Acad Sci USA. 2001; 98:12620–12623. [PubMed: 11606740]
18. Stavnezer J, Guikema JE, Schrader CE. Mechanism and regulation of class switch recombination. Annu Rev Immunol. 2008; 26:261–292. [PubMed: 18370922]
19. Ma L, Wortis HH, Kenter AL. Two new isotype-specific switching activities detected for Ig class switching. J Immunol. 2002; 168:2835–2846. [PubMed: 11884453]
20. Shanmugam A, Shi M-J, Yauch L, Stavnezer J, Kenter AL. Evidence for class-specific factors in immunoglobulin isotype switching. J Exp Med. 2000; 191:1365–1380. [PubMed: 10770803]
21. Wuerffel R, Wang L, Grigera F, Manis J, Selsing E, Perlot T, Alt FW, Cogne M, Pinaud E, Kenter AL. S-S synapsis during class switch recombination is promoted by distantly located transcriptional elements and activation-induced deaminase. Immunity. 2007; 27:711–722. [PubMed: 17980632]

22. Wang L, Whang N, Wuerffel R, Kenter AL. AID-dependent histone acetylation is detected in immunoglobulin S regions. J Exp Med. 2006; 203:215–226. [PubMed: 16418396]
23. Wuerffel RA, Ma L, Kenter AL. NF-kappa B p50-dependent in vivo footprints at Ig S gamma 3 DNA are correlated with mu—>gamma 3 switch recombination. J Immunol. 2001; 166:4552–4559. [PubMed: 11254712]
24. Chu CC, Paul WE, Max EE. Quantitation of immunoglobulin μ-γ 1 heavy chain switch region recombination by a digestion-circularization polymerase chain reaction method. Proc Natl Acad Sci USA. 1992; 89:6978–6982. [PubMed: 1495989]
25. Sakai E, Bottaro A, Davidson L, Sleckman BP, Alt FW. Recombination and transcription of the endogenous Ig heavy chain locus is effected by the Ig heavy chain intronic enhancer core region in the absence of the matrix attachment regions. Proc Natl Acad Sci USA. 1999; 96:1526–1531. [PubMed: 9990057]
26. Cogné M, Lansford R, Bottaro A, Zhang J, Gorman J, Young F, Cheng HL, Alt FW. A class switch control region at the 3′ end of the immunoglobulin heavy chain locus. Cell. 1994; 77:737–747. [PubMed: 8205622]
27. Sternberg N, Hoess R. The molecular genetics of bacteriophage P1. Annu Rev Genet. 1983; 17:123–154. [PubMed: 6364958]
28. Severinson E, Fernandez C, Stavnezer J. Induction of germ-line immunoglobulin heavy chain transcripts by mitogens and interleukins prior to switch recombination. Eur J Immunol. 1990; 20:1079–1084. [PubMed: 1972677]
29. Hummel M, Berry JK, Dunnick W. Switch region content of hybridomas: the two spleen cell Igh loci tend to rearrange to the same isotype. J Immunol. 1987; 138:3539–3548. [PubMed: 3106486]
30. Radbruch A, Müller W, Rajewsky K. Class switch recombination is IgG1 specific on active and inactive IgH loci of IgG1-secreting B-cell blasts. Proc Natl Acad Sci USA. 1986; 83:3954–3957. [PubMed: 3086872]
31. Winter E, Krawinkel U, Radbruch A. Directed Ig class switch recombination in activated murine B cells. EMBO J. 1987; 6:1663–1671. [PubMed: 3038529]
32. Yu K, Chedin F, Hsieh CL, Wilson TE, Lieber MR. R-loops at immunoglobulin class switch regions in the chromosomes of stimulated B cells. Nat Immunol. 2003; 4:442–451. [PubMed: 12679812]
33. Pinaud E, Khamlichi AA, Le Morvan C, Drouet M, Nalesso V, Le Bert M, Cogné M. Localization of the 3′ IgH locus elements that effect long-distance regulation of class switch recombination. Immunity. 2001; 15:187–199. [PubMed: 11520455]
34. Manis JP, Dudley D, Kaylor L, Alt FW. IgH class switch recombination to IgG1 in DNA-PKcs-deficient B cells. Immunity. 2002; 16:607–617. [PubMed: 11970883]
35. Zarrin AA, Goff PH, Senger K, Alt FW. Sgamma3 switch sequences function in place of endogenous Sgamma1 to mediate antibody class switching. J Exp Med. 2008; 205:1567–1572. [PubMed: 18541713]

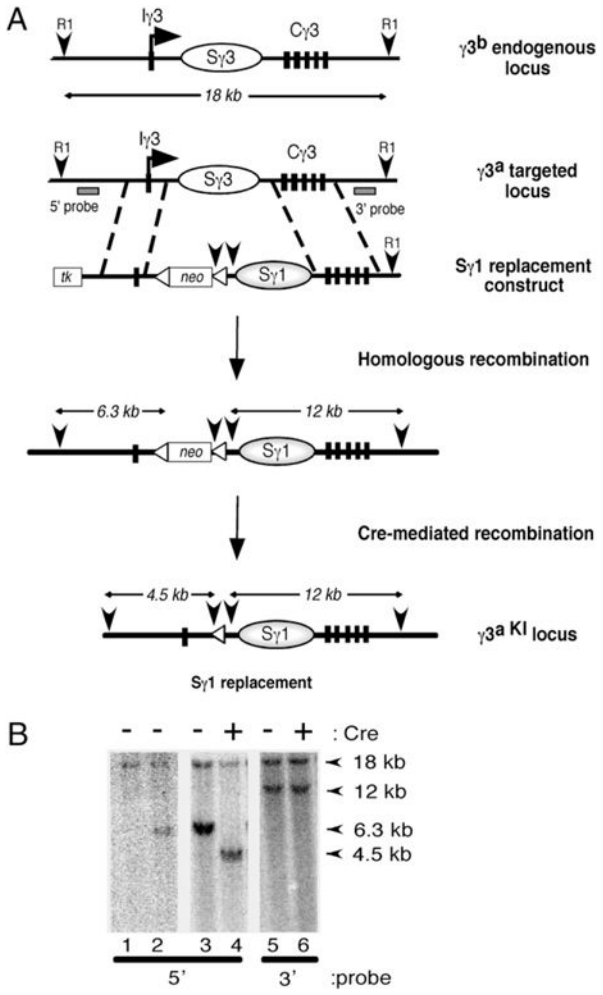

FIGURE 1.

Targeted replacement of the endogenous Sγ3[a] region. *A*, Insertion of Sγ1 into the γ3 locus. Genomic organization of the mouse Sγ3 loci on the targeted a allele (γ3[a]) or the WT b allele (γ3[b]). Vertical arrow heads R1, EcoRI; open triangles, *loxP* sites; tk, gene encoding the thymidine kinase; neo, neomycine resistance gene; rectangular blocks, Iγ3 and Cγ3; horizontal arrows, Iγ3 promoter; ovals, S regions (WT or targeted); and rectangular bars, probes for Southern analysis. The arrow at Iγ3 indicates the physiological orientation of transcription. *B*, Southern blot analysis of genomic DNA digested with EcoRI and hybridized with the 5′ probe (*lanes 1–4*) or 3′ probe (*lanes 5* and *6*). The 5′ probe on F1 ES cells detects 18-kb bands that represent the endogenous γ3 locus from both the a and b alleles. Following Cre-mediated deletion of the neo gene, the 5′ but not the 3′ homology arm is further reduced in size from 6.3-4.5 kb.

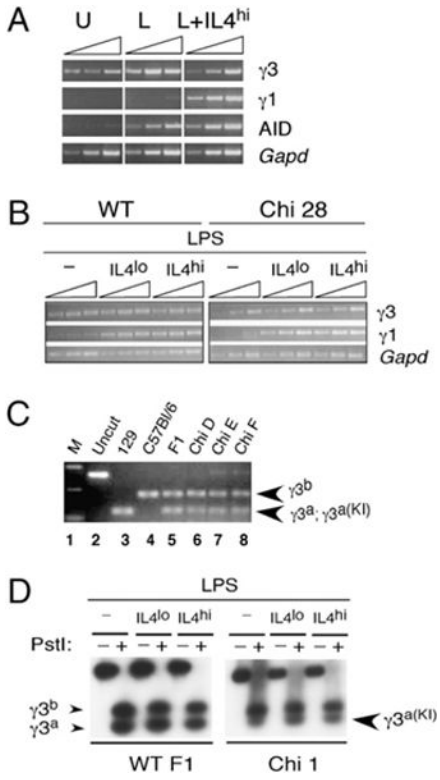

FIGURE 2.

Expression of γ3 GLT from intact and Sγ1 replacement alleles. GLT γ3, γ1, and AID expression were analyzed by semiquantitative RT-PCR using cDNAs derived from purified B cells or splenocytes that were either unstimulated (U) or activated with LPS (L) alone or LPS plus IL-4^{lo} (1 ng/ml) or LPS plus IL-4^{hi} (10 ng/ml) for 48 h. RT-PCR analyses of the *Gapd* or *Hprt* transcripts were used as loading controls. *A*, Purified B cells were unstimulated or stimulated and analyzed as indicated. *B*, WT F1 and chimeric (Chi 28) splenocyte cultures, activated as indicated, and then analyzed for γ3 or γ1 GLT expression. *C*, LPS-activated WT F1 and chimeric (Chi D, E, F) splenocyte cultures are analyzed for γ3 GLTs. Allele-specific products were distinguished by PstI digestion, which generates 180- and 125-bp restriction fragments derived from the C57/B6 (b) and 129 (a) alleles, respectively. Samples in *lanes 3–7* were digested with PstI. Samples are m.w. marker, M (*lane 1*), intact γ3 GLT (*lane 2*), and γ3 GLT from the I29 a allele (*lane 3*), the C57BL/6 b allele (*lane 4*), the 129 × C57BL/6 (F1) a and b alleles (*lane 5*), and Chi mice (*lanes 6–8*). *D*, WT F1 and chimeric (Chi 1) splenocyte cultures activated as indicated were assessed for allele-specific γ3 GLT by RT-PCR followed by Southern blot analysis.

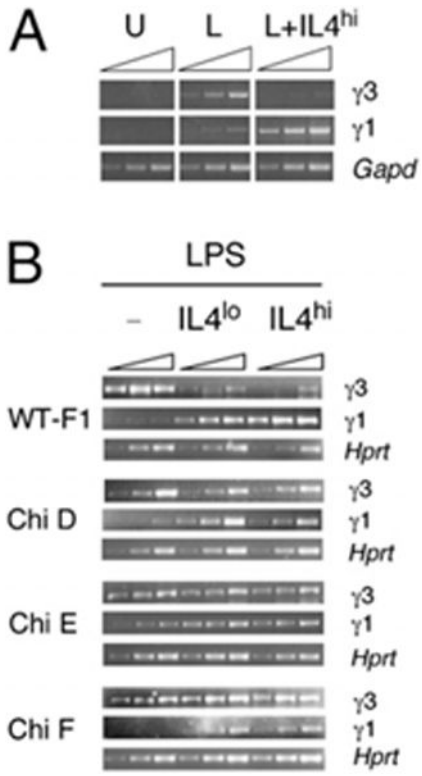

FIGURE 3.

Active μ→γ3 CSR in Sγ1 replacement splenocytes following LPS plus IL-4 induction. Purified B cells (*A*) or splenocytes from C57BL/6 × 129 (WT-F1) or Sγ1 replacement chimeric mice (*B*) were cultured for 5 d with LPS (L) in the presence or absence of IL-4^{lo} or IL-4^{hi}, as indicated. PST Iμ-Cγ3 and Iμ-Cγ1 were analyzed by semiquantitative RT-PCR. RT-PCR analyses of the *Gapd* or *Hprt* transcripts were used as loading controls. *A*, Purified B cells were unstimulated (U) or stimulated and analyzed as indicated. *B*, WT-F1 and chimeric (Chi D, E, F) splenocyte cultures, activated as indicated, and then analyzed for γ3 or γ1 PST expression.

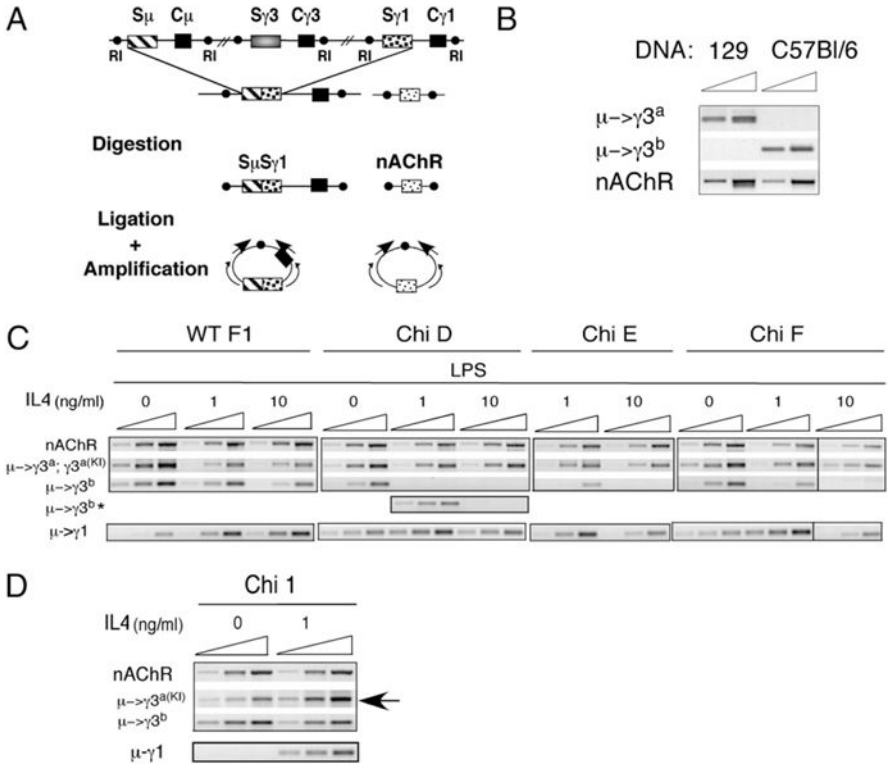

FIGURE 4.

DC-PCR analysis demonstrates that μ→γ3 CSR occurs on the Sγ1 replacement allele in response to LPS plus IL-4 activation. *A*, The DC-PCR strategy for detection of CSR at the endogenous γ3 locus is schematically illustrated. EcoRI sites (RI) flank the 5′ and 3′ ends of the S regions. Genomic DNA is digested with EcoRI and ligated under low concentration conditions that favor fragment circularization. The positions and orientations of the nested primer sets are shown postligation. The *nAChR* gene is used as a control. *B*, Allele-specific μ→γ3 DC-PCR is demonstrated using allele-specific primers and genomic DNA from the 129 a allele (μ→$\gamma3^{a}$) or C57BL/6 b allele (μ→$\gamma3^{b}$) mice. *C* and *D*, DC-PCR analysis of DNA from splenocytes from WT F1 and three independent chimeras (Chi D, E, F) that were stimulated with LPS alone or in the presence of LPS and IL-4^{lo} or IL-4^{hi} for 5 d. All DC-PCR products were harvested at 26, 29, and 32 cycles. *C*, Allele-specific μ→$\gamma3^{a}$ (WT) or μ→$\gamma3^{a(KI)}$ (Sγ1 replacement allele) and μ→$\gamma3^{b}$ (intact b allele) and μ→γ1 (WT a and b alleles) DC-PCR products. Templates were concentrated 5-fold and reanalyzed for the intact b allele as indicated (μ→$\gamma3^{b}$p). *D*, Allele-specific DC-PCR products μ→$\gamma3^{a(KI)}$, μ→$\gamma3^{b}$, or μ→γ1 for Chi 1.

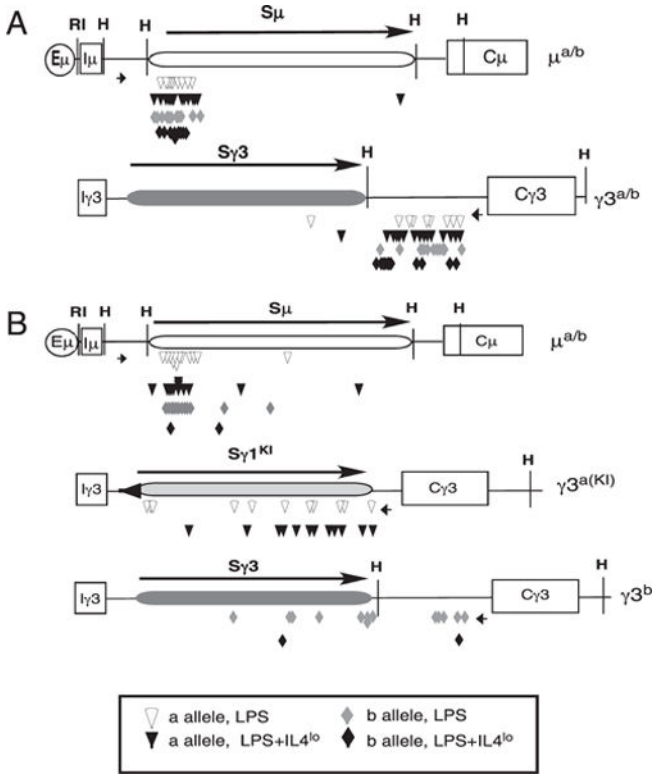

FIGURE 5.

S/S junction frequency analysis indicates IL-4–induced targeting of the $\gamma 3^{a(KI)}$ allele for $\mu \rightarrow \gamma 3$ CSR. Splenocytes were stimulated with LPS in the presence or absence of IL-4^{lo} for 5 d. S-S junctions from WT F1 (*A*) and chimeric (*B*) mice were amplified from genomic DNA using primers located 5′ of Sμ and in the Sγ3-Cγ3 intron as indicated by the arrows under each locus schematic. The locations of the recombination breakpoints were determined by DNA sequence analysis of the cloned PCR products and are indicated by the symbols beneath the locus diagrams. S-S junction sequences are shown in Supplemental Figs. 2 and 3 and are analyzed in Table I. In the Sγ1 replacement allele, indicated as $\gamma 3^{a(KI)}$, the remaining *loxP* site is shown by the black triangle upstream of the Sγ1 replacement region.

Table I

Switch junction analyses

	WT				Chimeras			
	Sμ^a-Sγ3^a	**Sμ^b-Sγ3^b**	***p* Value^a**	***n*^{b}**	**Sμ^a-Sγ1^{KI}**	**Sμ^b-Sγ3^b**	***p* Value^a**	***n*^{b}**
LPS	9	11	NS	20	11	13	NS	24
LPS plus IL-4^{lo}	12	9	NS	21	9	1	>0.011	10

[a] *p* values were calculated using a χ^2 analysis.

[b] *n* indicates the number of unique junctions analyzed.